Astronomy & Astrophysics

XMM-Newton observation of the Be/neutron star system RX J0146.9+6121: a soft X-ray excess in a low luminosity accreting pulsar[★]

N. La Palombara and S. Mereghetti

INAF – Istituto di Astrofisica Spaziale e Fisica Cosmica Milano, via Bassini 15, 20133 Milano, Italy
e-mail: nicola@iasf-milano.inaf.it

ABSTRACT

We report on the *XMM-Newton* observation of the Be/neutron star X-ray binary system RX J0146.9+6121, a long period (~23 m) pulsar in the NGC 663 open cluster. The X-ray luminosity decreased by a factor of two compared to the last observation carried out in 1998, reaching a level of ~1×10^{34} erg s^{-1}, the lowest ever observed in this source. The spectral analysis reveals the presence of a significant excess at low energies over the main power-law spectral component. The soft excess can be described by a black-body spectrum with a temperature of about 1 keV and an emitting region with a radius of ~140 m. Although the current data do not permit us to ascertain whether the soft excess is pulsed or not, its properties are consistent with emission from the neutron star polar cap. This is the third detection of a soft excess in a low luminosity (~1×10^{34} erg s^{-1}) pulsar, the others being X Per and 3A 0535+262, suggesting that such a spectral component, observed to date in higher luminosity systems, is a common feature of accreting X-ray pulsars. The results of these three sources indicate that, in low luminosity systems, the soft excess tends to have a higher temperature and a smaller surface area than in the high luminosity ones.

Key words. stars: individual: RX J0146.9+6121 – X-rays: binaries

1. Introduction

High Mass X-Ray Binaries (HMXRBs) are binary systems consisting of a neutron star (NS) or, less frequently, a black hole, accreting matter from a high mass early type star. Based on the nature of the mass donor star, either a supergiant of O/B spectral type or a Be star, HMXRBs can be divided in two subgroups showing different variability properties. HMXRBs with supergiant companions tend to be persistent sources, although some of them display high and low states with X-ray flux varying by large factor (~100 or more). On the other hand, neutron star Be X-ray binaries (BeXRBs) are generally transient sources, due to the long term variability of the equatorial discs surrounding Be stars and/or the orbital eccentricity. For both subgroups, when the compact object is a NS, the X-ray spectra are well described by a rather flat power-law between 0.1 and 10 keV (photon index ~1) followed by a high-energy cutoff.

With the advent of imaging X-ray satellites a large number of BeXRB systems has been discovered in the Small Magellanic Cloud (Haberl & Sasaki 2000; Israel et al. 2000; Yokogawa et al. 2003; Macomb et al. 2003; Sasaki et al. 2003; Haberl & Pietsch 2004). The observation of these sources, unaffected by the high interstellar absorption present in the Galactic plane, makes it possible to study in detail their X-ray spectra, extending down to energies of a few hundred eV. This has allowed investigators to discover that most of them have a marked soft excess above the power-law model (Nagase 2002; Haberl & Pietsch 2005).

RX J0146.9+6121 is a BeXRB hosting a neutron star characterized by a rotational period of about 23 min, among the longest observed in X-ray pulsars. The pulsations were discovered with non-imaging instruments on board EXOSAT and initially attributed to a different nearby source (White et al. 1987). Subsequent observations clarified the picture (Mereghetti et al. 1993; Hellier 1994) and led to the optical identification of RX J0146.9+6121 with the B0 IIIe star LS I +61° 235 (Coe et al. 1993). This star is a member of the open cluster NGC 663 (Tapia et al. 1991; Fabregat et al. 1996; Pigulski et al. 2001) for which a distance in the range between 2 and 2.5 kpc has been derived (Kharchenko et al. 2005; Pandey et al. 2005). In the following we adopt $d = 2.5$ kpc. Due to its relatively short distance, RX J0146.9+6121 is not much absorbed and is therefore a good target to investigate the properties of the soft X-ray emission in a Galactic source. Here we present the results of a recent observation obtained with the *XMM-Newton* satellite, providing the most sensitive observation of this source ever obtained below 2 keV.

2. Observations and data reduction

RX J0146.9+6121 was observed by *XMM-Newton* between 22:40 UT of 2004 January 14 and 10:20 UT of 2004 January 15. Since the main target was the NGC 663 open cluster, RX J0146.9+6121 was detected at an off-axis angle of 9.3′. The three *EPIC* instruments, i.e. the *pn* camera (Strüder et al. 2001) and the *MOS1* and *MOS2* cameras (Turner et al. 2001), were active and operated in *Full Frame* mode. For all of them, the Medium thickness filter was used.

[★] This work is based on observations obtained with *XMM-Newton*, an ESA science mission with instruments and contributions directly funded by ESA Member States and NASA.
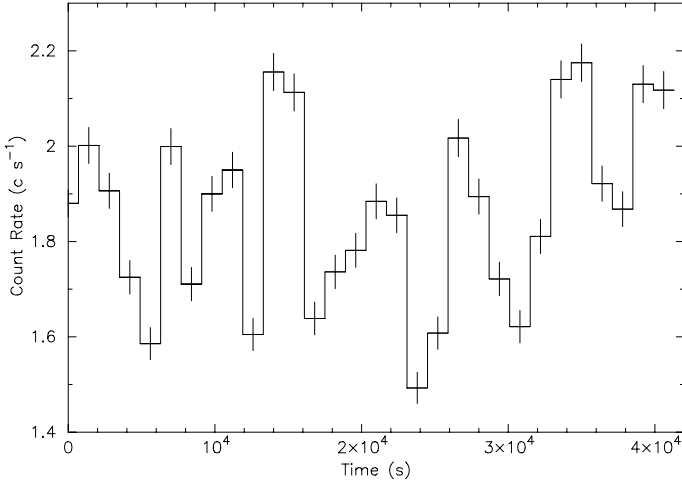
Fig. 1. Background subtracted light curve of RX J0146.9+6121 in the energy range 0.15−10 keV, with a time bin of 1.4 ks (i.e. 1 pulse period).
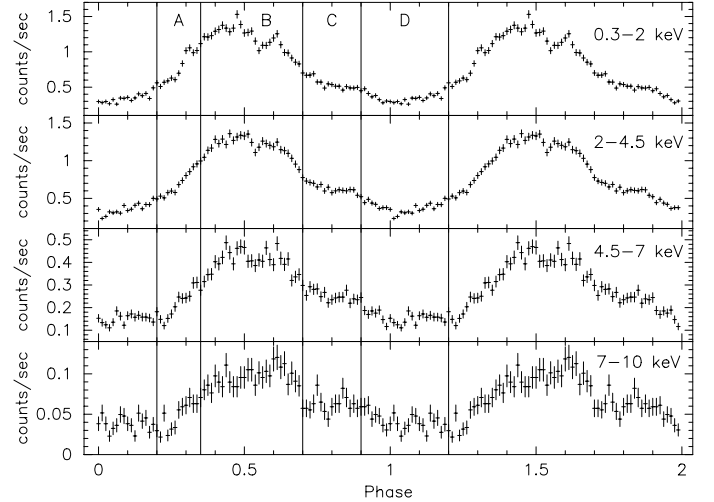

Fig. 2. Background subtracted light curves of RX J0146.9+6121 in the energy ranges 0.3−2, 2−4.5, 4.5−7 and 7−10 keV, folded at the best-fit period of 1396.14 s. The vertical lines indicate the phase intervals used for the spectral analysis.

Fig. 3. Hardness ratio of the two light curves of RX J0146.9+6121 in the energy ranges 0.3−2 and 2−10 keV, as a function of the pulse phase. The HR values are obtained by folding the light curves at the best-fit period of 1396.14 s. The pulse period is divided in 10 phase bins, which are identified by progressive numbers.

We used version 6.1 of the *XMM-Newton Science Analysis System* (*SAS*) to process the event files. After the standard pipeline processing of the data, we looked for possible periods of high instrumental background, due to flares of soft protons with energies less than a few hundred keV. We found that the first ~15 ks of the observation were affected by a soft-proton contamination. However, since RX J0146.9+6121 was detected with a count-rate (~1 cts s^{-1}) much higher than that of the background, the soft-protons during the bad time intervals have a negligible effect on the source spectral and timing analysis (their count rate in the source extraction area is less than 0.01 cts s^{-1}). Hence for our analysis we used the data of the whole observation, corresponding to exposure times of 35.4 and 41.2 ks in the *pn* and *MOS* cameras, respectively.

3. Timing analysis

During our observation some flux changes on an ~hour timescale were present, as shown by the background subtracted light curve plotted in Fig. 1. This is based on the data in the 0.15−10 keV range obtained from the three EPIC cameras. A bin size of 1.4 ks, corresponding to one spin period, has been chosen to avoid the effects due to the periodic pulsations. Variations up to ~20% around the average level of ~1.9 cts s^{-1} are evident.

To obtain a measure of the pulse period, we converted the times of arrival to the solar system barycenter and performed a folding analysis using the source events of three cameras. By fitting the χ^2 versus trial period curve with the appropriate sinc function as described in Leahy (1987), we derived a period of 1396.14 ± 0.25 s. In Fig. 2 we show the folded light curves in four energy intervals (0.3−2, 2−4.5, 4.5−7 and 7−10 keV) chosen to allow a direct comparison with the light curves previously derived with *RossiXTE* data (Mereghetti et al. 2000). The pulse profile, characterized by a broad peak, is clearly energy-dependent, with the maximum shifting from phase ~0.4−0.5 at $E < 2$ keV to phase ~0.6 at $E > 7$ keV.

The hardness ratio (HR) between the light curves above and below 2 keV, reported in Fig. 3, is characterized by a slow and regular increase from its minimum to its maximum value, followed by a rather irregular decrease. This plot, where we have divided the pulse period in ten phase intervals, shows that there is not a simple correlation between the hardness and the total count rate: we observe the same HR value at completely
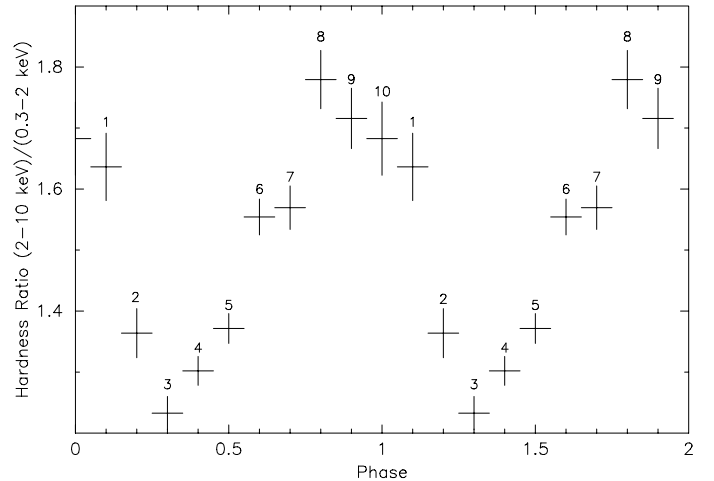
different count rate levels, but also very different HR values for the same count rate. This indicates that the spectral hardness of RX J0146.9+6121 does not depend in a simple way on its flux level.

4. Spectral analysis

For the source spectra we used an extraction radius of 30″ around the source position in the case of the *MOS2* and *pn* cameras; for the *MOS1* camera the extraction radius was reduced to 15″, since the source was imaged close to a CCD gap. We checked with the *SAS* task *epatplot* that no event pile-up affected our data, then we accumulated all the events with pattern range 0−4 (i.e. mono- and bi-pixel events) and 0−12 (i.e. from 1 to 4 pixel events) for the *pn* and the two *MOS* cameras, respectively. The background spectra were accumulated on large circular areas with no sources and radius of 210″ and 120″ for the *MOS1* and the *MOS2* camera, respectively. For the *pn* camera
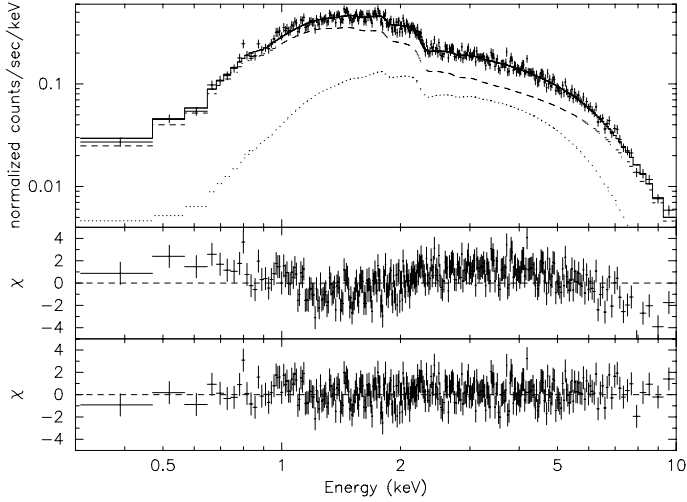
Fig. 4. *Top panel*: *pn* spectrum of RX J0146.9+6121 with the best-fit power-law (*dashed line*) plus black-body (*dotted line*) model. *Middle panel*: residuals (in units of σ) between data and model in the case of the single power-law. *Bottom panel*: residuals in the case of the power-law plus black-body.

the background spectrum was extracted from a circular region of the same radius and at the same CCD rows of the source region. We generated ad hoc response matrices and ancillary files using the *SAS* tasks *rmfgen* and *arfgen*. All spectra were rebinned with a minimum of 30 counts per bin and fitted in the energy range $0.3-10$ keV using *XSPEC* 11.3.2.

After checking that separate fits of the three spectra gave consistent results, we fitted the spectra from the three cameras simultaneously in order to increase the count statistics and to reduce the uncertainties. The fit with an absorbed power-law yielded $N_H = (6.24 \pm 0.14) \times 10^{21}$ cm^{-2} and photon index $\Gamma = 1.36 \pm 0.02$, but with large residuals and χ_ν^2/d.o.f. = 1.283/1480[1]. The addition of a blackbody component improved the fit quality significantly (Fig. 4): we obtained $N_H = (5.09^{+0.24}_{-0.23}) \times 10^{21}$ cm^{-2}, $\Gamma = 1.34^{+0.05}_{-0.06}$ and $kT_{BB} = 1.11^{+0.07}_{-0.06}$ keV, with χ_ν^2/d.o.f. = 1.036/1478. The emission surface of the thermal component has a radius $R_{BB} = 140^{+17}_{-14}$ m (for $d = 2.5$ kpc). The unabsorbed flux in the energy range $0.3-10$ keV is $f_X \sim 2 \times 10^{-11}$ erg cm^{-2} s^{-1}, about 24% of which is due to the blackbody component.

We also attempted to fit the soft part of the spectra with other emission models, such as *mekal*, thermal bremsstrahlung and broken power-law. In all these cases the results were worse than those obtained with the blackbody model, since the reduced chi-squared was higher, the residuals were larger and/or the best-fit parameter values were unrealistic.

We did not find significant evidence for emission lines. By adding Gaussian components at various energies to the above model, we estimated upper limits of the order of 150 eV for the equivalent width of lines in the $6-7$ keV energy range.

5. Phase-resolved spectroscopy

Prompted by the results described above, we performed a phase-resolved spectroscopy in order to study in more detail the source behavior. We defined phase 0 by matching the folded light curve to that observed in 1996 with *RossiXTE* and extracted the background subtracted spectra for the same four phase intervals used

[1] Errors are at a 90% confidence level for a single interesting parameter.

Table 1. Best-fit spectral parameters for the phase-resolved spectroscopy of RX J0146.9+6121, in the case of the independent fit of the four spectra. Errors are at a 90% confidence level for a single interesting parameter. N_H and kT_{BB} are measured in units of 10^{21} cm^{-2} and keV, respectively.

Spectral Parameter	Phase Interval			
	A	B	C	D
N_H	$4.8^{+0.4}_{-0.7}$	$5.4^{+0.4}_{-0.3}$	$5.0^{+0.8}_{-0.7}$	$3.6^{+0.6}_{-0.5}$
Γ	$1.47^{+0.19}_{-0.20}$	$1.39^{+0.09}_{-0.08}$	$1.31^{+0.35}_{-0.23}$	$1.06^{+0.11}_{-0.21}$
kT_{BB}	$0.98^{+0.08}_{-0.12}$	$1.05^{+0.10}_{-0.08}$	$1.34^{+0.17}_{-0.18}$	$1.21^{+0.21}_{-0.16}$
f_{TOT}^a	1.81	3.22	1.74	1.00
f_{PL}^a	1.34	2.52	1.10	0.70
	(74%)	(78%)	(63%)	(70%)
f_{BB}^a	0.47	0.70	0.64	0.30
	(26%)	(22%)	(37%)	(30%)
χ_ν^2/d.o.f.	0.972/308	1.021/992	1.085/352	1.131/328

[a] Unabsorbed flux in the energy range $0.3-10$ keV, in units of 10^{-11} erg cm^{-2} s^{-1}.

Table 2. Best-fit values for the black-body and power-law normalizations, when the four spectra are fitted simultaneously with common values of N_H $((5.8 \pm 0.1) \times 10^{21}$ cm^{-2}), Γ (1.60 ± 0.02) and kT_{BB} $(1.36^{+0.04}_{-0.03}$ keV). Errors are at a 90% confidence level for a single interesting parameter.

Spectral Parameter	Phase Interval			
	A	B	C	D
R_{BB}^a	76 ± 3	130 ± 2	121 ± 2	87 ± 2
I_{PL}^b	$2.24^{+0.07}_{-0.03}$	$3.25^{+0.05}_{-0.03}$	$1.32^{+0.03}_{-0.06}$	$0.89^{+0.01}_{-0.03}$
f_{TOT}^c	2.04	3.42	1.77	1.06
f_{PL}^c	1.69	2.46	1.00	0.67
	(83%)	(72%)	(56%)	(63%)
f_{BB}^c	0.35	0.96	0.77	0.39
	(17%)	(28%)	(44%)	(37%)

[a] Radius of the blackbody component (in metres) for a source distance of 2.5 kpc.
[b] Intensity of the power-law component in units of 10^{-3} ph cm^{-2} s^{-1} keV^{-1} at 1 keV.
[c] Unabsorbed flux in the energy range $0.3-10$ keV, in units of 10^{-11} erg cm^{-2} s^{-1}.

in Mereghetti et al. (2000) and indicated in Fig. 2. The first step was to fit all of them with the best-fit power law plus blackbody model of the phase averaged spectrum, leaving only the relative normalization factors free to vary. The ratios of the four spectra of each instrument to these renormalized average models show significant residuals and clearly demonstrate the spectral variability as a function of the pulse phase.

We then fitted the four spectra independently. In all cases, the absorbed power-law model was not satisfactory, while the addition of a black-body component significantly improved the fit. Therefore we used this model for all the spectra, leaving all the parameters free to vary: the results are reported in Table 1.

In order to investigate the relative variations of the two components with the period phase, we also simultaneously fitted the four spectra forcing common values for N_H, Γ and kT_{BB}. In this case we obtained $N_H = (5.8 \pm 0.1) \times 10^{21}$ cm^{-2}, $\Gamma_{PL} = 1.60 \pm 0.02$ and $kT_{BB} = 1.36^{+0.04}_{-0.03}$ keV, with χ_ν^2/d.o.f. = 1.117/1989; the corresponding normalization values are reported in Table 2. In this interpretation the spectral changes as a function of the phase are reproduced by the variations in the relative contribution of the two components.

Table 3. Best-fit values for the power-law parameters, when the four spectra are fitted simultaneously with common values of N_H (($6.1^{+0.3}_{-0.1}$)$\times$ 10^{21} cm^{-2}), kT_{BB} ($1.40^{+0.02}_{-0.04}$ keV) and R_{BB} (111^{+1}_{-4} m). Errors are at 90% confidence level for a single interesting parameter.

Spectral Parameter	Phase Interval			
	A	B	C	D
Γ	$1.98^{+0.03}_{-0.04}$	$1.57^{+0.02}_{-0.02}$	$1.56^{+0.04}_{-0.03}$	$2.63^{+0.13}_{-0.08}$
I_{PL}^a	$2.40^{+0.06}_{-0.06}$	$3.47^{+0.05}_{-0.04}$	$1.39^{+0.03}_{-0.05}$	$0.97^{+0.04}_{-0.05}$
f_{TOT}^b	2.08	3.43	1.81	1.19
f_{PL}^b	1.36	2.71	1.09	0.47
	(65%)	(79%)	(60%)	(40%)
f_{BB}^b	0.72	0.72	0.72	0.72
	(35%)	(21%)	(40%)	(60%)

[a] Intensity of the power-law component in units of 10^{-3} ph cm^{-2} s^{-1} keV^{-1} at 1 keV.
[b] Unabsorbed flux in the energy range 0.3−10 keV, in units of 10^{-11} erg cm^{-2} s^{-1}.

However, the above results do not necessarily imply that the soft component is pulsed. In fact an acceptable fit (χ_ν^2/d.o.f. = 1.097/1989) can also be obtained by imposing that the black-body component parameters be the same in the four spectra, as shown in Table 3.
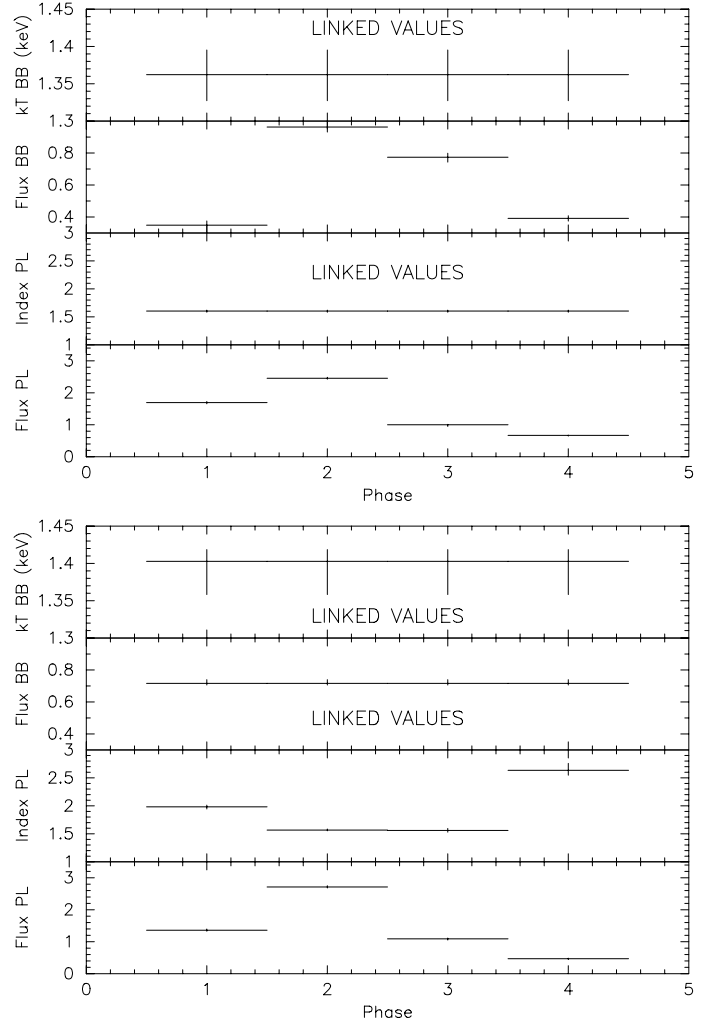
The above results are summarized in Fig. 5, where we show the pulse-phase dependence of the black-body temperature, the power-law photon index and the unabsorbed flux of the two components for both fits. Since they have a similar statistical quality, we can neither confirm nor deny that the thermal component is variable.

6. Discussion

The *XMM-Newton* data described here were obtained almost 6 years after the latest X-ray observation of RX J0146.9+6121, which was performed by *BeppoSAX* on 1998 February 3 (Mereghetti et al. 2000). Therefore it is interesting to compare our results with those obtained in the past. In Fig. 6 we show the long term evolution of the source spin period and luminosity since the time of the *EXOSAT* discovery in 1984. If we exclude the first observation, when the source was in outburst, a linear fit of all the periods gives a spin-up at an average rate of $\dot{P} = -(4.6^{+0.1}_{-0.2}) \times 10^{-8}$ s s^{-1}, similar to that measured until 1998. This result suggests that during the 6 years between the *BeppoSAX* and the *XMM-Newton* observations, the momentum transfer onto the neutron star has proceeded with no major changes. The flux detected by *XMM-Newton* corresponds to a luminosity of $\sim 1.5 \times 10^{34}$ erg s^{-1}, a factor ~ 2 lower than the minimum level observed in the previous years, indicating that, after the outburst of July 1997 (Haberl et al. 1998), RX J0146.9+6121 has been continuously fading.

Comparison with the *RossiXTE* results reported in Fig. 2 of Mereghetti et al. (2000) shows that, despite the luminosity variation, the shape of the pulse profiles in the energy interval common to the two instruments (2−10 keV) has not changed. The *XMM-Newton* data also confirm that, above 2 keV, there is a significant spectral softening in the initial rising part of the pulse (phase interval A).

The main advantage of the data reported here, with respect to previous observations of this source, is the better coverage of the energy range below 2 keV. In comparison to the *BeppoSAX* results, the phase averaged spectroscopy gives a smaller hydrogen column density: $N_H = (5.09^{+0.24}_{-0.23}) \times 10^{21}$ cm^{-2} instead of

Fig. 5. Pulse-phase dependence of the black-body temperature, the power-law photon index and the unabsorbed flux of the two components (in units of 10^{-11} erg cm^{-2} s^{-1}), in the case of a common temperature and index (*top*) and of a common black-body (*bottom*).
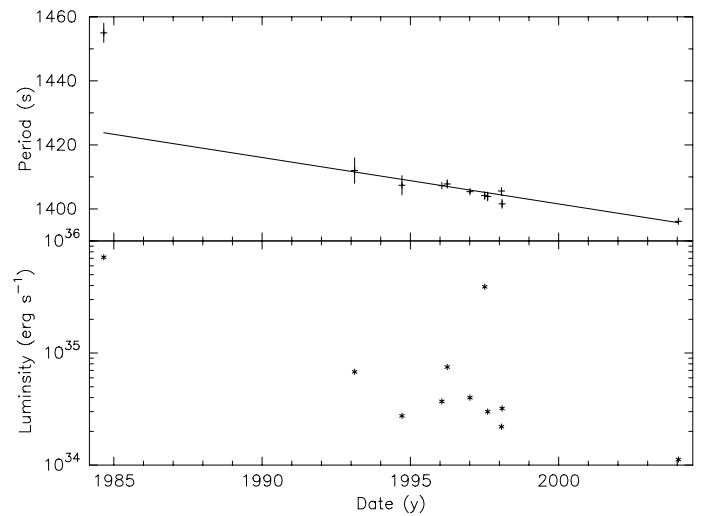
Fig. 6. Pulse period and luminosity history of RX J0146.9+6121 from 1984 August 27 to 2004 January 15. The solid line in the upper panel is the best-fit linear model of the reported values and has a slope $\dot{P} = -4.6 \times 10^{-8}$ s s^{-1}. The luminosities of the lower panel are based on the unabsorbed flux in the 2−10 keV energy range and on a source distance of 2.5 kpc.

$(1.2 \pm 0.3) \times 10^{22}$ cm^{-2}. This value is in better agreement with that expected from the optical observations which give $E(B - V) = 0.93$ (Reig et al. 1997). Assuming $A_V = 3.1 E(B - V)$ and the average relation $A_V = N_H \times 5.59 \times 10^{-22}$ cm^{-2} between optical extinction and X-ray absorption (Predehl & Schmitt 1995), this would predict $N_H = 5.16 \times 10^{21}$ cm^{-2}.

Moreover, we find evidence of a thermal component that was never observed before in this source. In recent years, similar soft excesses have been detected in several high mass X-ray binary pulsars. The properties of these sources are summarized in Table 4. Hickox et al. (2004) showed that a soft excess has been detected in all the X-ray pulsars with a sufficiently high flux and small absorption. In fact, most of the soft excess sources are at small distances and/or away from the Galactic plane (most of them are in the Magellanic Clouds). This suggests that the presence of a soft spectral component could be a very common, if not an ubiquitous, feature intrinsic to X-ray pulsars. These authors concluded that the origin of the soft component is related to the source total luminosity. When $L_X \geq 10^{38}$ erg s^{-1} the luminosity and the shape of the soft component can be explained only by reprocessing of hard X-rays from the neutron star by optically thick accreting material, most likely near the inner edge of the accretion disk. In less luminous sources, with $L_X \leq 10^{36}$ erg s^{-1}, the soft excess can be due to other processes, such as emission by photo-ionized or collisionally heated diffuse gas or thermal emission from the surface of the neutron star. Finally, in the sources of intermediate luminosity, either or both of these types of emission can be present.

In Fig. 7 we have plotted the X-ray luminosity versus interstellar absorption of the pulsars with a soft excess. We can see that RX J0146.9+6121, together with X Persei and 3A 0535+262, is at least one order of magnitude less luminous than all the other pulsars displaying a soft excess. We note that the ratio between the unabsorbed fluxes of the thermal and the power-law components in RX J0146.9+6121 agrees well with the average value measured in the other sources. However, unlike some of the other sources, the soft excess could be fitted only with a black-body component, while any other emission model was rejected.

Based on the results obtained by Hickox et al. (2004), the luminosity of RX J0146.9+6121 is too small for an interpretation of the soft excess in terms of reprocessing of the hard X-ray photons in optically thick accreting material. Moreover, both the thermal emission and the hard X-ray reprocessing in a diffuse, optically thin gas around the neutron star are unlikely, since these processes would not give a black-body spectrum. We therefore favor the interpretation of the soft excess in RX J0146.9+6121 as thermal emission from the neutron star polar cap. If we assume that the source is in the "accretor" status, with matter accretion on the NS surface, the blackbody emitting radius of $\sim$140 m is consistent with the expected size of the polar cap. In fact, if $M_{NS} = 1.4 \, M_\odot$ and $R_{NS} = 10^6$ cm, the source luminosity of $\sim 10^{34}$ erg s^{-1} implies an accretion rate $\dot{M} \sim 5 \times 10^{13}$ g s^{-1} and, adopting $B_{NS} = 10^{12}$ G, a magnetospheric radius $R_m \simeq 2.4 \times 10^9$ cm (Campana et al. 1998). In this case, based on the relation $R_{col} \sim R_{NS} (R_{NS}/R_m)^{0.5}$ (Hickox et al. 2004), we would obtain $R_{col} \sim 200$ m. If this description is correct, we would expect to observe some variability of the soft component along the pulse phase. From this point of view the phase-resolved spectroscopy provides no conclusive results, since it proves that both a variable and a constant thermal component can account for the observed spectral variability.

RX J0146.9+6121 is in many respects very similar to X Per and 3A 0535+262, which are very low luminosity Be/NS binary
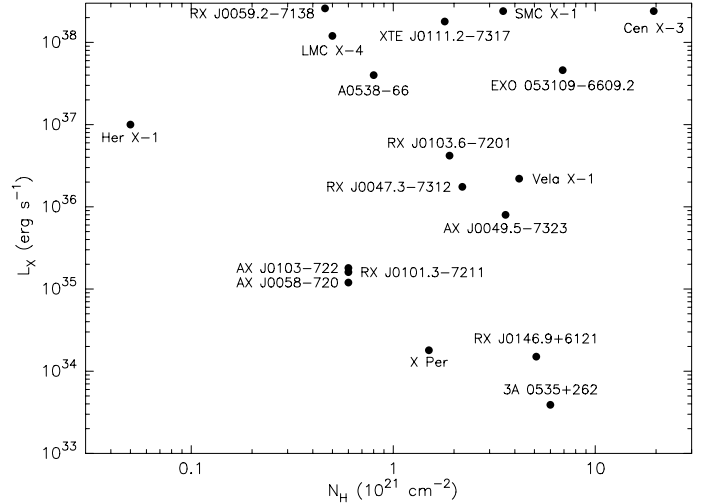
Fig. 7. Total X-ray luminosity of the sources of Table 4 as a function of the interstellar absorption.

with a long pulse period. The soft excesses of these sources have similar properties, since they tend to have a higher temperature (>1 keV) and a smaller emission radius ($\sim$0.1 km) compared to the soft excesses observed in high luminosity systems, which have a temperature of about 0.1 keV and an emission radius of a few hundred km. In these three low luminosity systems the soft excess contributes $25-35\%$ of the total flux (Coburn et al. 2001; Mukherjee & Paul 2005). Also in the case of X Per and 3A 0535+262 this excess has been attributed to the emission from the polar caps.

7. Conclusions

We have reported the analysis of the data collected by *XMM-Newton* in a $\sim$42 ks observation of the Be/neutron-star X-ray pulsar RX J0146.9+6121.

The unabsorbed flux corresponds to a source luminosity $L_X \sim 1 \times 10^{34}$ erg s^{-1} in the 2–10 keV energy range, about 50% lower than the lowest level ever observed from this source, indicating a monotonic source fading over long time scales.

Thanks to the high effective area of *XMM-Newton* also at low energies, we could perform the first accurate spectral study below 2 keV for this source. In the phase-averaged spectrum we have revealed the presence of a significant soft excess over the primary power-law component: this excess can be described by a black-body with $kT_{BB} \sim 1$ keV, while any attempt to fit it with a different emission model was unsuccessful.

The phase-resolved spectroscopy has confirmed the large spectral variability along the pulse period already observed above 2 keV. Unfortunately, with the current data, it is not possible to derive compelling results on the phase variability of the soft excess component. Although the emission below 2 keV is clearly pulsed and the low energy part of the spectrum varies with the phase, we have shown that such variations can be explained equally well by changes in the blackbody component or in the power law component alone.

Clearly the relatively small distance and low interstellar absorption toward RX J0146.9+6121 plays a role in the possibility of detecting a soft excess in such a low luminosity pulsar. Comparison with other X-ray binary pulsars shows that, so far, a soft excess has been detected only in much brighter sources. The data reported here support the hypothesis that a soft

Table 4. Orbital and spectral parameters for XBPs with a detected soft excess (SE).

Source[a]	Location	Distance (kpc)	Companion Star	P_{pulse} (s)	L_X^{b} (erg s^{-1}, keV)	Flux (erg cm^{-2} s^{-1})	N_H^{c} (10^{21} cm^{-2})	L_{SE}/L_X	SE model[d]	kT_{BB} (keV)	SE Pulses[e]
Her X-1[1]	Galaxy	~5	A7 V	1.24	1.0×10^{37} (0.3–10)	3.3×10^{-9}	0.05	0.04–0.10	BB, BB+LE	0.09–0.12	Yes
SMC X-1[2]	SMC	65	B0 Ib	0.7	2.4×10^{38} (0.7–10)	4.7×10^{-10}	2–5	0.036	BB, TB, SPL	0.15–0.18	Yes
LMC X-4[3]	LMC	50	O7III–OIV	13.5	1.2×10^{38} (0.7–10)	4.0×10^{-10}	~0.5	0.064	BB, BB+TB, COM, SPL	0.15	Yes
XTE J0111.2–7317[4]	SMC	65	B1 IVe	30.95	1.8×10^{38} (0.7–10)	3.6×10^{-10}	~0.10	0.31	SPL	...	Yes
RX J0059.2–7138[5]	SMC	65	B1 IIIe	2.76	2.6×10^{38} (0.1–10)	5.1×10^{-10}	1.8	–0.10	MEK, SPL	...	No
4U 1626–67[6]	Galaxy	?	Low–mass	7.7	$2.6 \times 10^{34} D_{kpc}^{2}$ (0.5–10)	2.2×10^{-10}	0.6	0.10	BB	0.34	No
Cen X-3[7]	Galaxy	~8	O6–O8 II	4.8	2.4×10^{38} (0.1–10)	3.2×10^{-8}	19.5	~0.7	BB	0.11	No
Vela X-1[8]	Galaxy	1.9	B0.5 Ib	283	2.2×10^{36} (2–10)	5.1×10^{-9}	4.2	~0.01	TB		No
X Per[9]	Galaxy	0.95	O9.5pe	837	1.8×10^{34} (0.3–10)	1.7×10^{-10}	1.5	0.24	BB	1.45	?
EXO 053109–6609.2[10]	LMC	50	B0.7 Ve	13.7	4.6×10^{37} (0.2–10)	1.5×10^{-10}	6.9	?	MEK+PL		Yes
A 0538–66[11]	LMC	50	B2 IIIe	0.069	4.0×10^{37} (0.1–2.4)	1.3×10^{-10}	0.8	?	BB, TB	~0.2	?
RX J0047.3–7312[12]	SMC	65	B2e	263	$1.5, 2. \times 10^{36}$ (0.7–10)	$3.0, 4.0 \times 10^{-12}$	0.96, 3.4	0.03–0.09, 0.68	BB	0.6, 2.2	Yes
RX J0101.3–7211[13]	SMC	65	Be	452	1.6×10^{35} (0.3–10)	3.2×10^{-13}	0.6	?	MEK		?
RX J0103.6–7201[14]	SMC	65	O5 Ve	1323	$0.8–7.5 \times 10^{36}$ (0.2–10)	$1.6–14.8 \times 10^{-12}$	1.9	?	MEK		No
AX J0049.5–7323[15]	SMC	65	B2 Ve	751	$7–9 \times 10^{35}$ (0.2–10)	$1.4–1.8 \times 10^{-12}$	3.6	?	?		Yes
AX J0058–720[13]	SMC	65	Be	281	1.2×10^{35} (0.3–10)	2.4×10^{-13}	0.6	?	MEK		Yes
AX J0103–722[13]	SMC	65	B0 IV	342	1.8×10^{35} (0.3–10)	3.6×10^{-13}	0.6	?	MEK		Yes
3A 0535+262[16]	Galaxy	2.0	O9.7 IIIe	103.4	3.9×10^{33} (2–10)	8.2×10^{-12}	6.0	0.35	BB	1.33	?
RX J0146.9+6121	Galaxy	2.5	B0 IIIe	1395	1.5×10^{34} (0.3–10)	2.0×10^{-11}	5.1	0.25	BB	1.11	?

[a] References: (1) dal Fiume et al. (1998), Endo et al. (2000), Ramsay et al. (2002); (2) Woo et al. (1995), Paul et al. (2002); (3) Woo et al. (1996), La Barbera et al. (2001), Naik & Paul (2004); (4) Yokogawa et al. (2000b); (5) Kohno et al. (2000); (6) Schulz et al. (2001); (7) Burderi et al. (2000); (8) Haberl (1994), Orlandini et al. (1998), Kreykenbohm et al. (2002); (9) di Salvo et al. (1998), Coburn et al. (2001); (10) Haberl et al. (2003); (11) Mavromatakis & Haberl (1993); (12) The two set of values are base on Ueno et al. (2004) and Majid et al. (2004), respectively; (13) Sasaki et al. (2003); (14)Sasaki et al. (2003), Haberl & Pietsch (2005); (15) Yokogawa et al. (2000a), Haberl & Pietsch (2004); (16) Mukherjee & Paul (2005).
[b] For each source the reference energy range is also reported.
[c] The reported values refer only to the interstellar absorption, not to the source intrinsic absorption.
[d] Spectral models used for the soft excess are: BB = blackbody; TB = thermal bremsstrahlung; SPL = soft power-law or broken power-law; MEK = MEKAL thin thermal model; COM = Comptonization model; LE = broad low-energy line emission. Commas indicate separate fits, plus signs indicate fits with two components.
[e] Pulsation of the emission component that traces the soft excess.

thermal component is a ubiquitous emission feature of this class of sources. In this sense, it would be very interesting to use the large collecting area of *XMM-Newton* in long observations of the faintest and longest period Be binaries, both in the SMC and in the Milky Way, such as, for example, the persistent low luminosity systems RX J0440.9+4431 and RX J1037.5−5647 (Reig & Roche 1999).

References

Burderi, L., Di Salvo, T., Robba, N. R., La Barbera, A., & Guainazzi, M. 2000, ApJ, 530, 429

Campana, S., Colpi, M., Mereghetti, S., Stella, L., & Tavani, M. 1998, A&AR, 8, 279

Coburn, W., Heindl, W. A., Gruber, D. E., et al. 2001, ApJ, 552, 738

Coe, M. J., Everall, C., Norton, A. J., et al. 1993, MNRAS, 261, 599

dal Fiume, D., Orlandini, M., Cusumano, G., et al. 1998, A&A, 329, L41

di Salvo, T., Burderi, L., Robba, N. R., & Guainazzi, M. 1998, ApJ, 509, 897

Endo, T., Nagase, F., & Mihara, T. 2000, PASJ, 52, 223

Fabregat, J., Torrejon, J. M., Reig, P., et al. 1996, A&AS, 119, 271

Haberl, F. 1994, A&A, 288, 791

Haberl, F., & Sasaki, M. 2000, A&A, 359, 573

Haberl, F., & Pietsch, W. 2004, A&A, 414, 667

Haberl, F., & Pietsch, W. 2005, A&A, 438, 211

Haberl, F., Angelini, L., & Motch, C. 1998, A&A, 335, 587

Haberl, F., Dennerl, K., & Pietsch, W. 2003, A&A, 406, 471

Hellier, C. 1994, MNRAS, 271, L21

Hickox, R. C., Narayan, R., & Kallman, T. R. 2004, ApJ, 614, 881

Israel, G. L., Campana, S., Covino, S., et al. 2000, ApJ, 531, L131

Kharchenko, N. V., Piskunov, A. E., Röser, S., Schilbach, E., & Scholz, R.-D. 2005, A&A, 438, 1163

Kohno, M., Yokogawa, J., & Koyama, K. 2000, PASJ, 52, 299

Kreykenbohm, I., Coburn, W., Wilms, J., et al. 2002, A&A, 395, 129

La Barbera, A., Burderi, L., Di Salvo, T., Iaria, R., & Robba, N. R. 2001, ApJ, 553, 375

Leahy, D. A. 1987, A&A, 180, 275

Macomb, D. J., Fox, D. W., Lamb, R. C., & Prince, T. A. 2003, ApJ, 584, L79

Majid, W. A., Lamb, R. C., & Macomb, D. J. 2004, ApJ, 609, 133

Mavromatakis, F., & Haberl, F. 1993, A&A, 274, 304

Mereghetti, S., Stella, L., & de Nile, F. 1993, A&A, 278, L23

Mereghetti, S., Tiengo, A., Israel, G. L., & Stella, L. 2000, A&A, 354, 567

Mukherjee, U., & Paul, B. 2005, A&A, 431, 667

Nagase, F. 2002, J. Astrophys. Astron., 23, 59

Naik, S., & Paul, B. 2004, ApJ, 600, 351

Orlandini, M., dal Fiume, D., Frontera, F., et al. 1998, A&A, 332, 121

Pandey, A. K., Upadhyay, K., Ogura, K., et al. 2005, MNRAS, 358, 1290

Paul, B., Nagase, F., Endo, T., et al. 2002, ApJ, 579, 411

Pigulski, A., Kopacki, G., & Kołaczkowski, Z. 2001, A&A, 376, 144

Predehl, P., & Schmitt, J. H. M. M. 1995, A&A, 293, 889

Ramsay, G., Zane, S., Jimenez-Garate, M. A., den Herder, J.-W., & Hailey, C. J. 2002, MNRAS, 337, 1185

Reig, P., Fabregat, J., Coe, M. J., et al. 1997, A&A, 322, 183

Reig, P., & Roche, P. 1999, MNRAS, 306, 100

Sasaki, M., Pietsch, W., & Haberl, F. 2003, A&A, 403, 901

Schulz, N. S., Chakrabarty, D., Marshall, H. L., et al. 2001, ApJ, 563, 941

Strüder, L., Briel, U., Dennerl, K., et al. 2001, A&A, 365, L18

Tapia, M., Costero, R., Echevarria, J., & Roth, M. 1991, MNRAS, 253, 649

Turner, M. J. L., Abbey, A., Arnaud, M., et al. 2001, A&A, 365, L27

Ueno, M., Yamaguchi, H., Takagi, S.-I., Yokogawa, J., & Koyama, K. 2004, PASJ, 56, 175

White, N. E., Mason, K. O., Giommi, P., et al. 1987, MNRAS, 226, 645

Woo, J. W., Clark, G. W., Blondin, J. M., Kallman, T. R., & Nagase, F. 1995, ApJ, 445, 896

Woo, J. W., Clark, G. W., Levine, A. M., Corbet, R. H. D., & Nagase, F. 1996, ApJ, 467, 811

Yokogawa, J., Imanishi, K., Tsujimoto, M., Koyama, K., & Nishiuchi, M. 2003, PASJ, 55, 161

Yokogawa, J., Imanishi, K., Ueno, M., & Koyama, K. 2000a, PASJ, 52, L73

Yokogawa, J., Paul, B., Ozaki, M., et al. 2000b, ApJ, 539, 191